International Journal of Heat and Fluid Flow 30 (2009) 1193–1201

Contents lists available at ScienceDirect

International Journal of Heat and Fluid Flow

journal homepage: www.elsevier.com/locate/ijhff

A gas jet superposition model for CFD modeling of group-hole nozzle sprays

Sung Wook Park [a], Rolf D. Reitz [b,*]

[a] Department of Mechanical Engineering, Hanyang University, Seoul 133-791, Republic of Korea
[b] Engine Research Center, University of Wisconsin–Madison, Madison, 1500 Engineering Drive, WI 53706, USA

ARTICLE INFO

Article history:
Received 17 February 2009
Received in revised form 25 April 2009
Accepted 4 June 2009
Available online 7 July 2009

Keywords:
Gas jet superposition
Spray modeling
Group-hole nozzles

ABSTRACT

In the present study, a jet superposition modeling approach is explored to model group-hole nozzle sprays, in which multiple spray jets interact with each other. An equation to estimate the merged jet velocity from each of the individual jets was derived based on momentum conservation for equivalent gas jets. Diverging and converging group-hole nozzles were also considered. The model was implemented as a sub-grid-scale submodel in a Lagrangian Drop–Eulerian Gas CFD model for spray predictions. Spray tip penetration predicted using the present superposition model was validated against experimental results for parallel, diverging and converging group-hole nozzles as a function of the angle between the two holes at various injection and ambient pressures. The results show that spray tip penetration decreases as the group hole diverging or converging angle increases. However, the spray penetration of the converging group-hole nozzle arrangement is more sensitive to the angle between the two holes compared to diverging nozzle because the radial momentum component is converted to axial momentum during the jet–jet impingement process in the converging group-hole nozzle case. The modeling results also indicate that for converging group-hole nozzles the merged sprays become ellipsoidal in cross-section far downstream of the nozzle exit with larger converging angles, indicating increased air entrainment.

1. Introduction

The use of the group-hole fuel injector nozzle concept has attracted significant interest in diesel engine research because it has potential to reduce droplet size without sacrificing spray tip penetration or mixing with the ambient air. The simplest group-hole nozzle configuration consists of two parallel injector hole passages with minimal spacing between the holes (Park and Reitz, 2008, 2009; Tokudo et al., 2005; Nishida et al., 2006; Moon et al., 2008). The group-hole nozzle is thought to increase the amount of entrained air, which is important for high equivalence ratio combustion concepts, such as low temperature combustion (Kimura et al., 2002) and stoichiometric diesel combustion (Lee et al., 2007, 2006). Therefore, many researchers have investigated the spray and combustion characteristics of diesel engines equipped with group-hole nozzles.

The effects of hole spacing and the orientation angles of group-hole nozzle passages on the spray size distributions and evaporation were studied by Nishida et al. (2006) using laser absorption scattering methods. Moon et al. (2008) explored the ignition and combustion characteristics of wall-impinging sprays injected from a group-hole nozzle for various spray included angles. Park and Reitz (Park and Reitz, 2008) performed numerical calculations of the effects of nozzle-hole configurations on fuel consumption and emission characteristics and found that the group-hole nozzle has potential benefits for high equivalence ratio operation (e.g., high EGR (Exhaust Gas Recirculation)) cases. However, possible effects of numerical grid-size dependency of the results were not considered in their study, Numerical parameter effects are an important consideration in modeling group-hole nozzle sprays for engine applications since CFD mesh sizes are necessarily much larger than the nozzle hole sizes, and spray interaction processes are not resolved.

It is well known that spray characteristics such as spray penetration and size distributions can be highly dependent on the numerical mesh grid-size and time step (Abani et al., 2008b,c) and coarse meshes can lead to inaccurate estimates of the droplet-gas relative velocity and drop collision processes. In order to reduce grid- and time-step dependencies, Abani et al. (2008c) introduced a so-called "gas jet submodel" which calculates the ambient gas velocity as a function of distance from the nozzle tip in the unresolved near-nozzle region using results from an equivalent gas jet injection, instead of using the CFD-predicted gas velocities. The equivalent gas jet parameters are those suggested by Abraham (1996) and Schlichting (1976). In addition, Abani et al. (2008a–c) used a ROI (radius-of-influence) collision model and a mean collision time model to reduce numerical dependencies in the collision model (Abani et al., 2008c).

* Corresponding author. Tel.: +1 608 262 0145; fax: +1 608 262 6707.
E-mail address: reitz@engr.wisc.edu (R.D. Reitz).

0142-727X/$ - see front matter © 2009 Elsevier Inc. All rights reserved.
doi:10.1016/j.ijheatfluidflow.2009.06.002

Nomenclature

d_{noz}	nozzle diameter	SMD	Sauter mean diameter
d_{col}	mean collision time step	U	velocity vector of droplet
K_{entr}	entrainment gas constant	U_{inj}	instantaneous injection velocity
N_{cv}	number of droplets within the control volume	$U_{max,cell}$	maximum drop velocity within the cell
PDPA	phase Doppler particle analyzer	V_{axis}	gas jet velocity in spray axis
R	radial distance from nozzle axis	Z	axial distance from nozzle tip
ROI	radius-of-influence		

Park et al. (2009) used the new spray models of Abani et al. (2008b) (i.e., the gas jet model, ROI collision model, and the mean collision time model) to reduce numerical dependencies in modeling group-hole nozzles. They validated the models using experimental spray penetration and SMD (Sauter mean diameter) distributions and successfully demonstrated reduced numerical dependencies in comparison to conventional spray models. Furthermore it was shown that hole-location dependency with respect to the position of the nozzle within the injection cell itself is also an important issue in modeling group-hole nozzles, and it was also reduced with new spray models. They assumed that the equivalent gas jet velocity of a group-hole nozzle is identical to that of single-hole nozzle with the same nozzle cross-sectional area. This assumption is reasonable because previous studies had shown that sprays issuing from group-hole nozzles have very similar tip penetrations to those from a single-hole nozzle with equivalent hole area (Tokudo et al., 2005; Nishida et al., 2006; Zhang et al., 2003). However, this assumption is clearly only applicable to the parallel group-hole nozzle configuration with very small inter-hole spacing. It has been shown by Zhang et al. (2003) that the spray characteristics of a converging or diverging group-hole nozzle depend on the angle between the two hole passages. In order to apply the gas jet submodel methodology to converging/diverging group-hole nozzle sprays, it is necessary to describe the flows resulting from merged jets. Accordingly, in the present study, a superposition methodology is proposed for use with the gas jet approach that is based on momentum conservation. The submodel was implemented in a CFD code, and validated using experimentally measured spray tip penetrations.

2. Model formulation

In the present study a modified version of the KIVA-3V release 2 code (Amsden, 1999) was used as the CFD model. In addition, the gas jet submodel, radius-of-influence collision model, and mean collision model were applied in order to reduce grid-size and time-step dependencies of the CFD code predictions (Park et al., 2009). For modeling converging and diverging group-hole nozzles, a gas jet-based superposition submodel was formulated, and was implemented and tested for use in CFD codes.

2.1. Grid-size and time-step independent spray models

As mentioned above, in order to reduce numerical dependencies, the new spray submodels proposed by Abani et al. (2008c) were used. In the gas jet submodel (Abani et al., 2008c; Park et al., 2009), the axial component of the gas phase velocity in the droplet momentum equation in each computational cell is specified using gas jet theory (Abani and Reitz, 2007; Abani et al., 2008a) instead of using the CFD solution in unresolved regions near the nozzle exit. This sub-grid-scale modeling methodology reduces the grid-size dependency which comes from inaccurate specification of the relative velocity between the gas and liquid phases. The gas jet velocity in the spray direction is given by

$$V_{axis} = \frac{3U_{inj}d_{noz}\sqrt{\frac{\rho_l}{\rho_g}}}{K_{entr}Z}\left(\frac{1}{\left(1+\frac{12R^2}{K_{entr}^2Z^2}\right)^2}\right) \quad (1)$$

where, U_{inj} is instantaneous injection velocity at the nozzle exit, d_{noz} is the nozzle exit hole diameter, and K_{entr} is an empirical gas entrainment constant determined to be 0.5, based on comparisons to experimental spray penetrations (Park et al., 2009). Z and R are the distance from the nozzle along the spray axis and the radial distance from the spray axis, respectively. When V_{gas} is higher than U_{inj}, V_{gas} is assumed to be equal to U_{inj}. The gas jet model is applied only during the injection event and the ambient gas velocity is given by the CFD prediction before or after injection.

The other source of grid-size dependency is inaccurate calculation of drop collision and coalescence processes because conventional collision models only consider drop parcels in the same computational cell as collision partners (Abani et al., 2008c). In the present study, the ROI (radius-of-influence) model was used that searches for collision partners such that if the distance between two droplets is shorter than a specified cut-off distance (i.e., the radius-of-influence), they are also considered as potential collision partners. In the present study, the radius-of-influence was selected to be 2 mm as suggested by Munnannur (2007) who noted that diesel spray simulations, the results are relatively insensitive to the cut-off distance once a large enough ROI is selected. In addi-

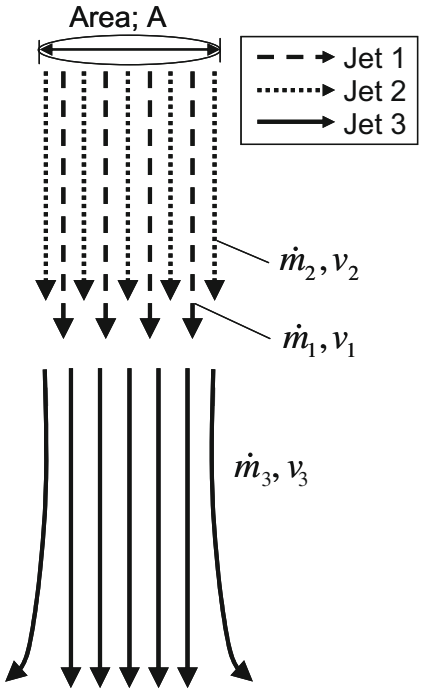

Fig. 1. Superposition of two parallel jets. Jet 1 and jet 2 are merged into jet 3 and $\dot{m}$ and v represent the mass flow rate and velocity of each jet.

tion, since the ROI is independent of the CFD mesh size, the grid dependency of the collision model is effectively eliminated.

The mean collision time submodel further reduces the numerical time-step dependency. Spray characteristics such as the mean droplet size can be significantly dependent on the time step because the collision and coalescence processes are calculated at each hydrodynamic time step in the conventional KIVA code, and Munnannur (2007) showed that SMD (Sauter mean diameter) increases as the time step decreases. Accordingly, a mean collision time step was introduced as

$$dt_{col} = \frac{0.4}{u_{max,cell}}\left(\frac{ROI}{N_{cv}^{1/3}}\right) \tag{2}$$

where, R_{inf} is the radius-of-influence, N_{cv} is the number of droplets within the control volume considered for resolution improvement and $u_{max,cell}$ is the maximum drop velocity within the computational domain. If the hydrodynamic time step is shorter that the mean collision time step, the collision calculations are by-passed until the elapsed time equals the mean collision time. If the hydrodynamic time step is longer that the mean collision time, the collision model is subcycled at the mean collision time step.

For the calculation of spray atomization and breakup, the KH (Kelvin–Helmholtz) breakup model was used for modeling the detachment of droplets from the intact liquid core. The RT (Kelvin–Helmholtz) breakup model was also used to describe secondary drop breakup in conjunction with the KH model, as suggested by Beale and Reitz (1999).

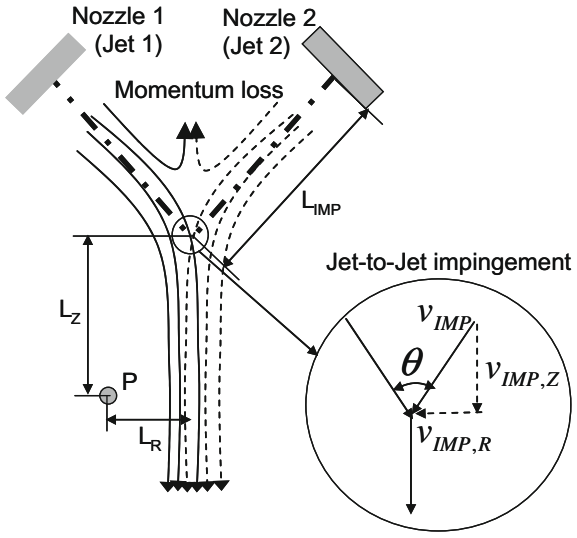

Fig. 2. Superposition of two converging jets. Jets collide at a distance of L_{IMP} from the nozzle tip.

2.2. Gas jet superposition model

In the group-hole nozzle concept, two holes are located closely spaced (e.g., 0.15–0.3 mm hole-to-hole centerline distance) and the two jets interact with each other right after emerging from the nozzles. Therefore, application of the gas jet model methodology to modeling group-hole nozzles requires superimposing the two flows. Fig. 1 depicts the superposition of two parallel gas jets. In this figure, jet 1 and jet 2 are merged to become jet 3 where the combined jets flow through the area, A.

In order to apply gas jet model to model gas jet spray, gas jet velocity of merged jet (v_3) is required. From momentum conservation,

$$\dot{m}_3 v_3 = \dot{m}_1 v_1 + \dot{m}_2 v_2 \tag{3}$$

where $\dot{m}$ and v indicate the mass flow rate and gas jet velocity, respectively, and subscripts 1 and 2 are the properties injected from nozzles 1 and 2, respectively. The fluid density and merged jet area are assumed to be the same at station 3. In this case, the emerged jet velocity, v_3, is derived in terms of v_1 and v_2 as

$$v_3 = \sqrt{v_1^2 + v_2^2} \tag{4}$$

For applying this model in a CFD code, the gas jet velocities from each hole (i.e., v_1 and v_2) at the injector nozzle exit must be supplied, as in modeling single-hole nozzles. Eq. (4) also can be derived from the Bernoulli equation by assuming that the superimposed jet pressures and potential energies at the impingement location are identical.

In cases of a diverging group-hole nozzle with angle between the two jets of θ, the effective jet velocity acting on the other jet can be estimated by multiplying by the component $\cos\theta$. Therefore, the jet velocity can be calculated as,

$$v_3 = \sqrt{v_1^2 + (v_2\cos\theta)^2} \quad \text{(for fluid issuing from nozzle 1)} \tag{5.1}$$

$$v_3 = \sqrt{(v_1\cos\theta)^2 + v_2^2} \quad \text{(for fluid from nozzle 2)} \tag{5.2}$$

For converging group-hole nozzle, impingement of two gas jets needs to considered in the model as shown in Fig. 2. In Fig. 2, jet 1 and jet 2 are issued from nozzle 1 and nozzle 2, respectively and they are impinged at the distance of L_{IMP} from nozzles. If parcel is located above L_{IMP}, that is, before impingement, the gas jet velocity for the parcel (v_{GAS}) is calculated by

$$v_{GAS} = \sqrt{v_1^2 + (v_2\cos\theta)^2} \quad \text{(for parcels issued from nozzle 1)} \tag{6.1}$$

$$v_{GAS} = \sqrt{(v_1\cos\theta)^2 + v_2^2} \quad \text{(for parcels issued from nozzle 2)} \tag{6.2}$$

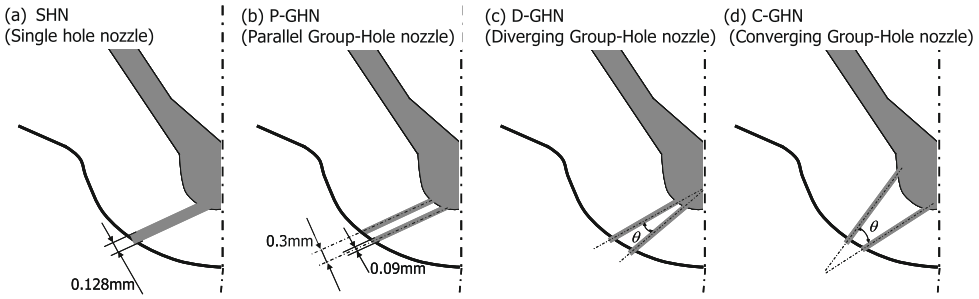

Fig. 3. Configurations of test nozzles (not to scale). In the case of group-hole nozzles, center-to-center distances between holes are 0.3 mm at the nozzle exit and the total hole areas of all nozzles are the same.

Eqs. (6) have the same form as Eqs. (5) because there no physical interaction (e.g., collision/coalescence) occurs between the two jets above the impingement point (L_{IMP}).

After impingement, the momentum loss due to impingement must be considered in calculating the merged jet velocity. In the present model, it is assumed that the momentum loss is proportional to the radial momentum component, as shown in Fig. 2. This is believed to be reasonable because thew axial momentum is conserved even during the impingement process. Considering the momentum lost by jet–jet impingement, the jet velocity loss is expressed as

$$v_{GAS,Loss} = v_{IMP} \times \sin(\theta/2) \times C_{CONV}. \quad (7)$$

where v_{IMP} is the jet velocity at the impingement point and C_{CONV} is a momentum conversion coefficient from radial to axial momentum flow components.

In order to estimate the jet velocity at a specific point (e.g., point P in Fig. 2), two jet velocities are calculated, one from jet 1, and the other from jet 2. For calculating each jet velocity, it is assumed that the axial distance from the nozzle exit is the length of the path travelled (i.e., $L_{IMP} + L_Z$), and the radial distance is the distance to the spray axis after impingement (i.e., L_R). With these axial and radial distances and equivalent gas jet velocity equation of Eq. (1), the jet velocity effecting point P ($v_{GAS,t}$) can be calculated. Note that the momentum loss due to jet–jet impingement is not considered in $v_{GAS,t}$. By considering the loss in jet velocity using Eq. (7) and superimposing the two jet velocities from jet 1 and jet 2 using Eq. (4), the jet velocity at point P is

$$v_{GAS,P} = \sqrt{2(v_{GAS,t} - v_{GAS,Loss})} \quad (6)$$

2.3. Calculation conditions

A uniform Cartesian hexagonal three-dimensional mesh was used for modeling group-hole nozzle sprays with a numerical grid cell size of $2.0 \times 2.0 \times 2.0$ mm^3. The sides of the calculation domain were equal to 150 mm in length and 60×60 mm^2 in plane area.

For the validation of the present jet superposition model, spray tip penetrations were compared to experimental results. Four different nozzle layouts were considered in the validations; a single-hole nozzle with 0.128 mm hole diameter, a parallel group-hole nozzle with two holes each of 0.09 mm hole diameter, a 3° converging, and a 3° diverging nozzle, as shown in Fig. 3. All nozzle layouts have the same total hole flow area. Ambient gas pressures were varied from atmospheric to 1.5 MPa with injection pressures ranging from 80 MPa to 150 MPa. In addition, the effect of converging group-hole nozzle configurations on spray shapes were studied over wide ranges of converging angle (up to 40°) to assess the effects of converging angle. Further details of the calculation conditions are listed in Table 1.

Table 1
Test conditions.

Fuel	Diesel fuel no. 2			
Time step (s)	1.0×10^{-6}			
Injection pressure (MPa)	80, 150			
Ambient conditions				
Pressure (MPa)	0.1	0.5	1.0	1.5
Density (kg/m^3)	1.12	5.61	11.23	16.85
Ambient gas	Nitrogen			
Discharge coefficient	0.8			

3. Experiments for model validation and CFD model inputs

For validating the present superposition model, jet tip penetrations were obtained from images from a spray visualization system, which consists of an Ar-ion laser, an ICCD camera, and a time delay generator. The Ar-ion laser illuminated the spray through the side window of the chamber and the camera captured bottom-viewed images of the spray. The spray tip penetration data were determined from the average of 100 injections.

A Bosch injection rate meter (Bosch, 1966) was used to provide the time-resolved injection profile and injection delay data. The measured pressure profiles were converted into injection mass profile with measurements of the total injected mass measured by a precision scale. The measured rate of injection data was used for specifying the injection velocities and for determining the nozzle discharge coefficients.

4. Results and discussion

The present superposition model was validated against spray penetration experimental data at various injection and ambient pressures, and the effect of nozzle converging or diverging angle on spray penetration and mean droplet size distributions were investigated.

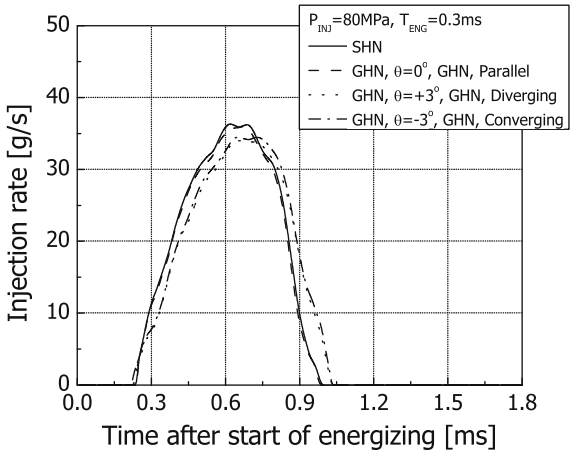

(a) P_{inj}=80MPa

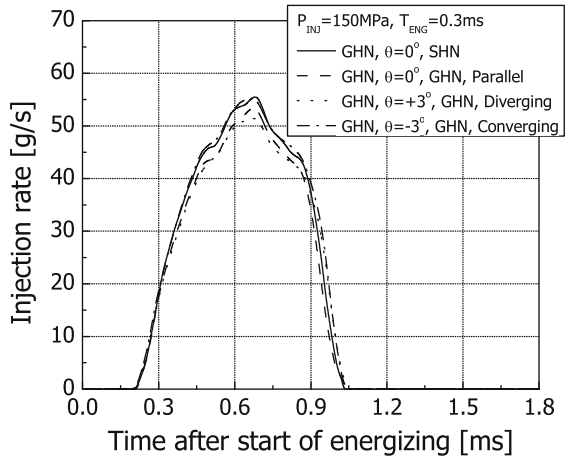

(b) P_{inj}=150MPa

Fig. 4. Injection rate and fuel mass per injection. Energizing durations of the injectors are the same up to 0.3 ms.

4.1. Effect of nozzle layout on rate of injection and determination of C_{CONV}

Fig. 4 shows measured rate of injection profiles for the various nozzle layouts, which have the same overall hole areas. With an energizing time of 3 ms, the real injection duration is around 0.9 ms at 150 MPa injection pressure. It can be seen that nozzle layout has little effect on the injection rate since the nozzles have the same overall hole area. The conversion coefficient (C_{CONV}) of Eq. (7), which controls the transfer of radial to axial momentum, was determined using experimental data of Iwabuchi et al. (1999). They investigated the effect of converging angle on spray penetration, as shown in Fig. 5. By comparing the normalized spray penetration to that of a parallel group-hole nozzle the conversion coefficient was determined to be 0.1.

Previous studies have shown that the spray tip penetration gets shorter and the spray cross-section becomes ellipsoidal as the converging angle increases due to the interactions between the two jets (Nishida et al., 2006; Gao et al., 2007). Therefore, the performance of the superposition model and its ability to predict spray shapes properly for converging group-hole nozzles was of interest. Fig. 6 shows effect of varying the converging angle from 0° to 40° in side- and bottom-view spray images at the end of injection for a 150 MPa injection pressure, 1.5 MPa ambient pressure injection. It is seen that the spray tip penetration is reduced, and the cross-section becomes ellipsoidal as the group-hole nozzle converging angle is increased, in agreement with experimental trends. The increased spray area indicates increased air entrainment into the spray.

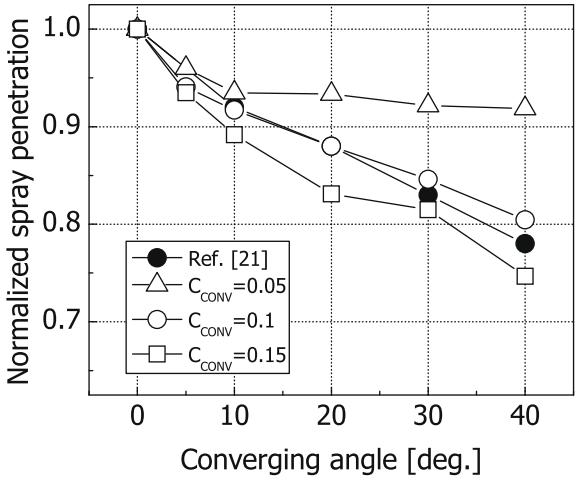

Fig. 5. Determination of conversion coefficient (C_{CONV}). Spray penetrations are normalized to that of the parallel nozzle at the end of injection (t_{asoi} = 0.9 ms).

4.2. Validation of the gas jet superimposition model and effect of angle between holes on spray characteristics

Fig. 7 shows the effect of inter-hole angle on spray tip penetrations for more modest converging and diverging angles with various injection and ambient conditions. The four nozzle layouts are referred to as the: single-hole nozzle (SHN), parallel (P-GHN), 3° diverging (D-GHN), and 3° converging (C-GHN) group-hole nozzles. The calculated tip penetrations are compared to the experimental data in Fig. 7, and can be seen to closely follow the experimental results. For both predicted and experimental results, the parallel group-hole nozzle has similar spray tip penetration to a single-hole nozzle with the same overall hole area, consistent also with previous studies (Tokudo et al., 2005; Nishida et al., 2006; Moon et al., 2008; Gao et al., 2007). The total injected momentum from the parallel group-hole nozzle is the same as that from the single-hole nozzle.

For all conditions in Fig. 7, the penetrations of the converging group-hole nozzle are also similar to those of the parallel group-hole nozzle, in spite of the momentum loss due to impingement. Considering that the inter-hole angle is minimal (i.e., 3°), the momentum loss by jet–jet impingement is also small. Therefore, the spray from a converging group-hole nozzle maintains similar momentum to that of the parallel nozzle. However, the diverging group-hole is seen to have a shorter spray penetration compared to either the parallel or converging group-hole nozzles. The fact

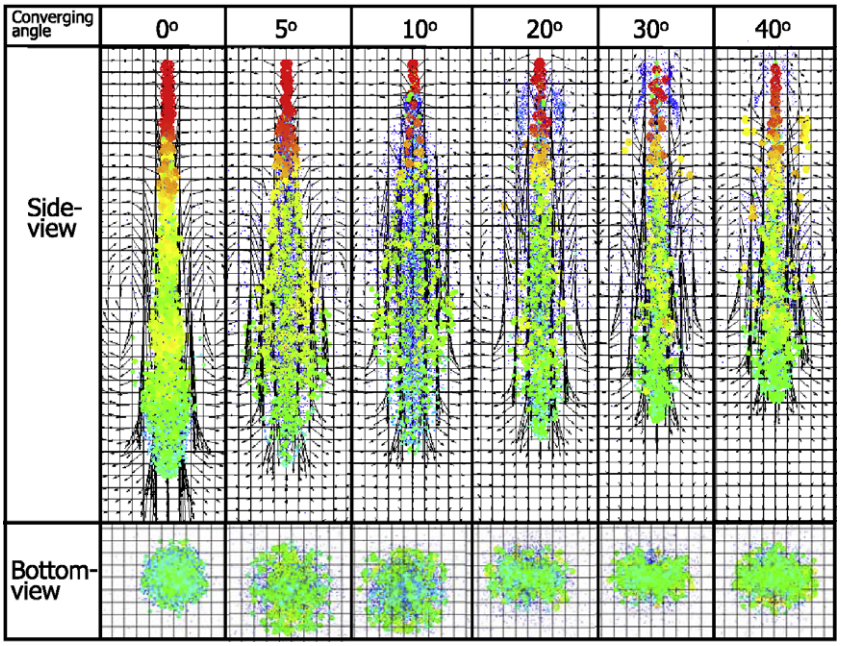

Fig. 6. Effect of group-hole nozzle converging angle on spray development (P_{amb} = 150 MPa, P_{amb} = 1.5 MPa). Spray images shown at end of injection (t_{asoi} = 0.9 ms).

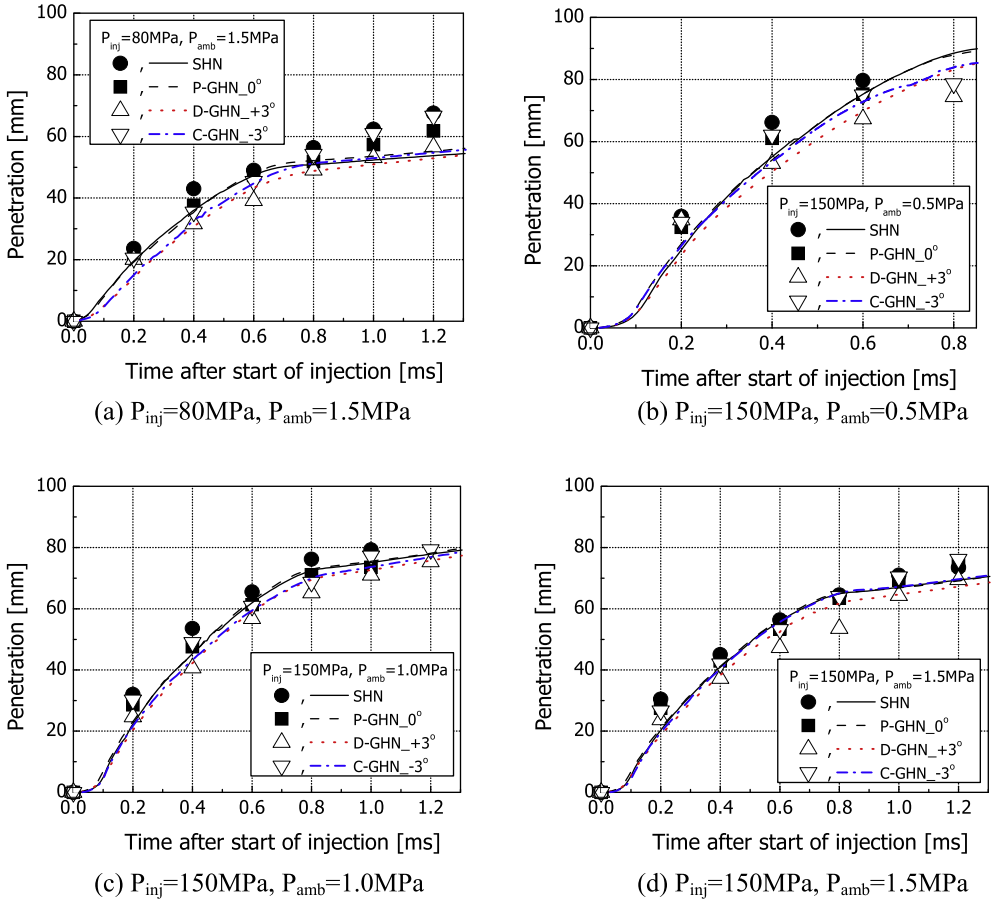

Fig. 7. Effect of group-nozzle layout on spray penetration for different injection and ambient pressures. Symbols and lines indicate experimental and calculation results, respectively.

that there is no momentum transfer from the radial to the axial direction in the diverging group-hole nozzle explains the shorter spray tip penetration seen in Fig. 7.

Calculated mean droplet size distributions for the various nozzle layouts are shown in Fig. 8. In this figure, overall SMD indicates the mean droplet size for all spray parcels in the calculation domain. Although there is no measured droplet size for validation, SMD distributions have been validated for parallel group-hole and single-hole nozzles in a previous study (Park et al., 2009) and showed reasonable agreement with measured data. At the low injection pressure and high ambient pressure of Fig. 8a, all the group-hole nozzle configurations feature a larger SMD distribution than the single-hole nozzle. It is evident that there is more active interaction between the droplets in the dense spray, near-nozzle region of a group-hole nozzle. Hence, coalescence collisions are expected to be more dominant than grazing droplet separations (Park et al., 2006; Lee and Reitz, 2001) at low Weber numbers (i.e., low injection pressure and high ambient pressure). Therefore active interaction between the droplets from group-hole nozzles increase SMD.

The results of Fig. 8b–d further explore the effect of ambient pressure on the overall SMD distribution. At 0.5 MPa ambient pressure (Fig. 8b), the converging group-hole nozzle shows similar SMD to the single-hole nozzle because separations and grazing collisions are promoted compared to case of Fig. 8a. However, as the ambient pressure increases, which promotes lower Weber numbers due to higher droplet drag effects, the SMD of the converging group-hole nozzle droplets becomes larger. In addition, that the collision impact parameter also has significant effect on droplet size distributions. Generally, impact parameters of parcels for converging group-hole nozzle are expected to be greater than those for parallel group-hole nozzle since the droplet streams are targeted toward each other. Collisions tend to separations rather than coalescences with greater impact parameters. In the diverging group-hole nozzle configuration, the droplets do not collide as frequently as in the converging group-hole nozzle case.

Fig. 9 shows the predicted spray shapes at the end of injection (t_{asoi} = 0.9 ms) for 150 MPa injection pressure and 1.5 MPa ambient pressure. It can be seen sprays issuing from parallel or diverging group-hole nozzles have fewer small droplets at the outer edge regions of the sprays due to active coalescences. However, in the converging group-hole nozzle, many small droplets are observed at the outer edge regions of the spray. This trend agrees with the overall SMD result seen in Fig. 8d.

Spray penetrations of diverging and converging group-hole nozzles with larger angles are shown in Fig. 10. Although there is no experimental data for these group-hole nozzles, the effect of diverging/converging angle on spray penetrations is predicted. As can be seen, spray penetration decreases as the diverging or converging nozzle angle increases. Furthermore, the spray penetrations of the diverging group-hole nozzle are more sensitive to angle between the two holes than those of the converging group-hole nozzle. In the present gas jet superposition submodel, most of the radial momentum is converted to axial momentum in the converging group-hole nozzle, which leads to longer spray penetration compared to that of the diverging group-hole nozzle with the same angle.

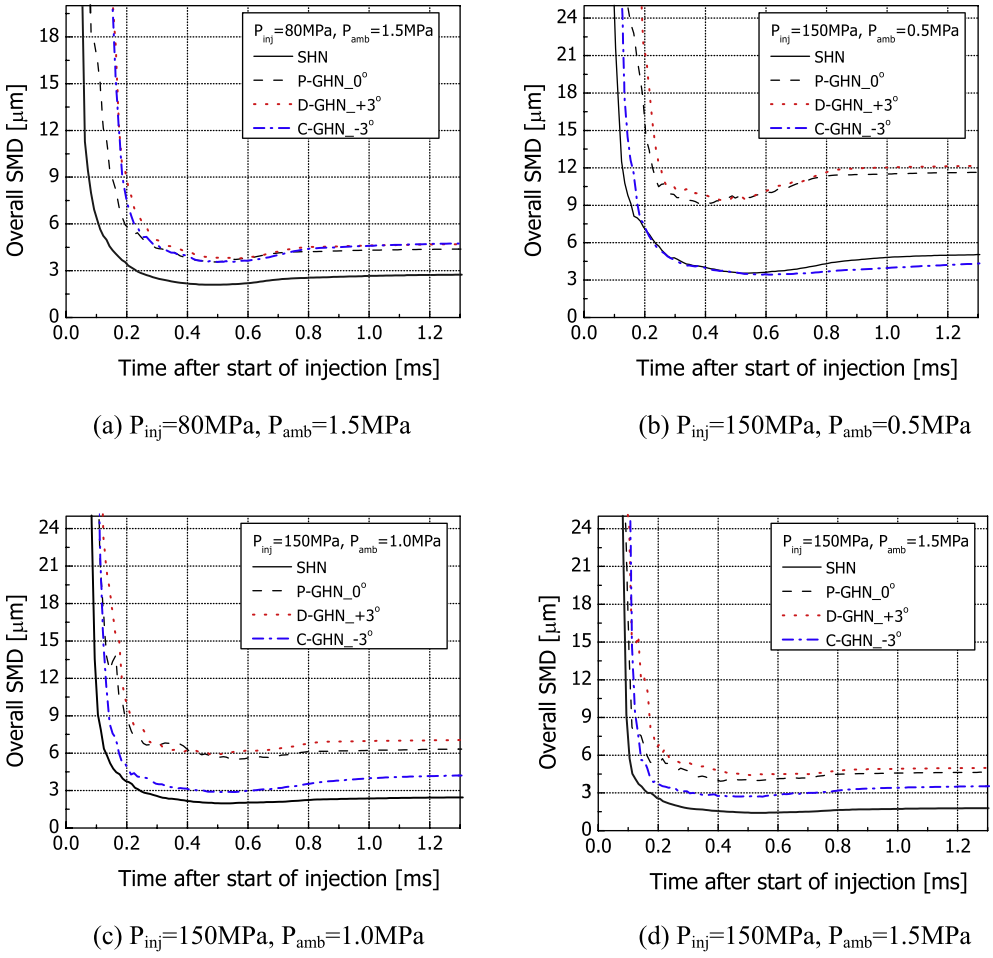

Fig. 8. Effect of group-hole nozzle layout and injection and ambient pressures on calculated overall SMD distributions.

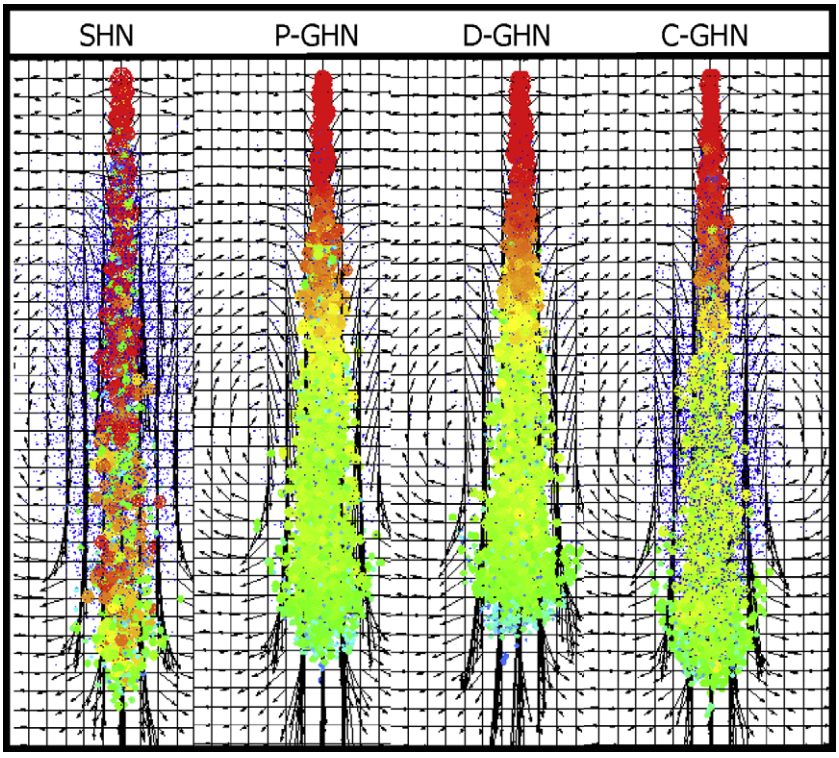

Fig. 9. Effect of group-hole nozzle layout on spray shape at the end of injection (t_{asoi} = 0.9 ms). Injection and ambient pressure are 150 MPa and 1.5 MPa, respectively.

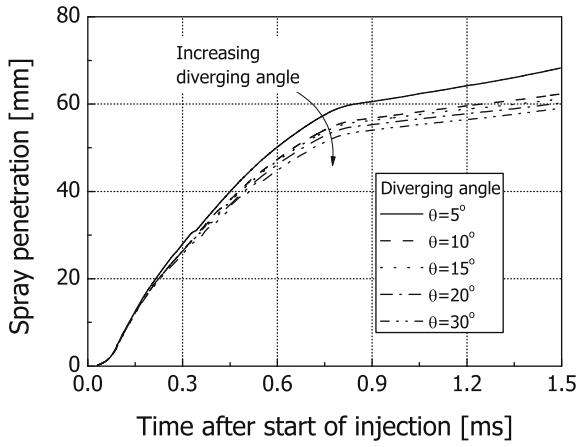

(a) Diverging group-hole nozzle

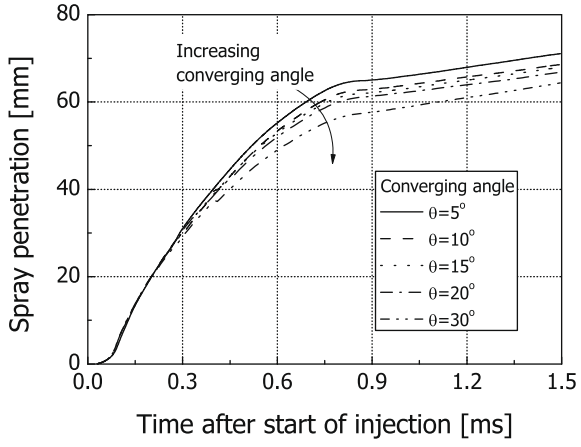

(b) Converging group-hole nozzle

Fig. 10. Effect of diverging/converging angle on spray penetration for 150 MPa injection pressure and 1.5 MPa ambient pressure (calculated results).

5. Conclusions

In the present study a jet superposition submodel is proposed for modeling group-hole nozzles in CFD simulations. This model is formulated based on momentum conservation, and was validated using experimental spray tip penetration data at various injection and ambient pressures. Using the model, the effect of group-hole nozzle diverging and converging angle on spray characteristics was investigated numerically. The following conclusions were drawn based on the results.

1. The merging of group-hole nozzle jets can be modeled by considering the superposition of the jet momenta. The model exploits the analogy that exists between gas jets and sprays with the same injected mass and momentum. When implemented in a CFD spray code, the proposed submodel provides good agreement with experimental spray tip penetration measurements at various injection and ambient pressures.
2. The present superposition submodel makes it possible to account for sub-grid-scale jet interaction processes that characterize parallel, converging and diverging group-hole nozzle configurations.
3. For converging group-hole nozzles, the spray tip penetration is decreased and the spray cross-section becomes ellipsoidal in shape as the converging angle is increased due to the effect of the interactions between the two jets, and this indicates increased air entrainment.
4. Based on the predicted drop sizes (SMD) of the group-hole nozzle sprays, it was seen that a converging group-hole nozzle provides similar drop sizes to a single-hole nozzle because separation collisions are promoted instead of coalescences as the injection pressure increases. However, as the ambient pressure is increased (leading to reduced drop Weber numbers due to higher drop drag), the drop SMD of the converging group-hole nozzle is increased compared to that of the diverging hole nozzle due to increased drop coalescence.
5. The converging group-hole nozzle has a longer spray tip penetration than the diverging group-hole nozzle due to the conversion of radial to axial momentum that occurs when the two jets impinge.

Acknowledgements

The authors gratefully acknowledge support for this work from Denso, Nippon Soken, General Motors Research & Development, the ERC Diesel Emissions Reduction Consortium member companies and the DOE LTC Consortium project DE-FC26-06NT42628.

References

Amsden, A.A., 1999. KIVA-3V Release 2, Improvement to KIVA-3V. Los Alamos National Laboratory. Report No. LA-UR-99-915.
Abani, N., Reitz, R.D., 2007. Unsteady turbulent round jets and vortex motion. Physics of Fluids 19, 125102.
Abani, N., Ghandhi, J.B., Reitz, R.D., 2008a. Vortex motion and unsteady turbulent jet penetration. In: Thermo and Fluid Dynamic Process in Diesel Engine (THIESEL) Conference, Spain.
Abani, N., Munnannur, A., Reitz, R.D., 2008b. Reduction of numerical parameter dependencies in diesel spray models. Journal of Engineering for Gas Turbines and Power 130, 032809.
Abani, N., Kokjohn, S., Park, S.W., Bergin, M., Munnannur, A., Ning, W., Sun, Y., Reitz, R.D., 2008. An improved spray model for reducing numerical parameter dependencies in diesel engine CFD Simulations. SAE Paper 2008-01-0970.
Abraham, J., 1996. Entrainment characteristics of transient jets. Numerical Heat Transfer Part A 30, 347–364.
Beale, J.C., Reitz, R.D., 1999. Modeling spray atomization Kelvin–Helmholtz/Rayleigh–Taylor hybrid model. Atomization and Sprays 9, 623–650.
Bosch, W., 1966. The fuel rate indicator: a new measuring instrument for display of the characteristics of individual injection. SAE Paper 660749.
Gao, J., Matshmoto, Y., Namba, M., Nishida, K., 2007. Group-hole nozzle effects on mixture formation and in-cylinder combustion processes in direct-injection diesel engines. SAE Paper 2007-01-4050.
Iwabuchi, Y., Kawai, K., Shoji, T., Takeda, Y., 1999. Trial of new concept diesel combustion system-premixed compression-ignited combustion. SAE Paper 1999-01-0185.
Kimura, S., Ogawa, H., Matsui, Y., Enomoto, Y., 2002. An experimental analysis of low-temperature and premixed combustion for simultaneous reduction of NO_x and particulate emissions in direct injection diesel engines. International Journal of Engine Research 3, 249–259.
Lee, C.S., Reitz, R.D., 2001. Effect of liquid properties on the breakup mechanism of high-speed liquid drops. Atomization and Sprays 11, 1–19.
Lee, S., Gonzalez, M.A.D., Reitz, R.D., 2006. Stoichiometric combustion in a HSDI diesel engine to allow use of a three-way exhaust catalyst. SAE Paper 2006-01-1148.
Lee, S., Gonzalez, M.A., Reitz, D.R.D., 2007. Effects of engine operating parameters on near stoichiometric diesel combustion characteristics. SAE Paper 2007-01-0121.
Moon, S., Gao, J., Nishida, K., Matsumoto, Y., Zhang, Y., 2008. Ignition and combustion characteristics of wall-impinging sprays injected by group-hole nozzles for direct-injection diesel engines. SAE Paper 2008-01-2469.
Munnannur, A., 2007. Droplet Collision Modeling in Multi-dimensional Engine Spray Computations, Ph.D. Thesis. Department of Mechanical Engineering, University of Wisconsin–Madison.
Nishida, K., Nomura, S., Matsumoto, Y., 2006. Spray and mixture properties of group-hole nozzle for D.I. diesel engine. In: Proceeding of ICLASS 2006, ICLASS06-171, Japan.
Park, S.W., Reitz, R.D., 2008. Modeling of the effect of injector nozzle-hole layout on diesel engine fuel consumption and emissions. Journal of Engineering for Gas Turbines and Power 130, 032805.
Park, S.W., Reitz, R.D., 2009. Optimization of fuel/air mixture formation for stoichiometric diesel combustion using 2-spray-angle group-hole nozzle. Fuel 88, 843–852.

Park, S.W., Kim, S., Lee, C.S., 2006. Breakup and atomization characteristics of mono-dispersed diesel droplets in a cross-flow air stream. International Journal of Multiphase Flow 32, 807–822.

Park, S.W., Abani, N., Reitz, R.D., Suh, H.K., Lee, C.S., 2009. Modeling of group-hole nozzle sprays using grid-size, hole-location, and time-step independent models. Atomization and Sprays 19 (6), 567–582.

Schlichting, H., 1976. Boundary Layer Theory. McGraw Hill, NY, USA.

Tokudo, H., Itoh, S., Kinugawa, M., 2005. Denso common rail technology to successfully meet future emission regulation. In: Proceedings of the 26th Vienna Motor Symposium, Austria.

Zhang, Y., Nishida, K., Nomura, S., Ito, T., 2003. Spray characteristics of group-hole nozzle for D.I. diesel engines. SAE Paper 2003-01-3115.